

UPCommons

Portal del coneixement obert de la UPC

<http://upcommons.upc.edu/e-prints>

Cristian Verdugo, Mohamed Atef Elsharty, Pedro Rodríguez. (2018) Integrated series transformer in cascade converters for photovoltaic energy systems. ECCE 2018: IEEE Energy Conversion Congress and Exposition: Portland, OR, USA: Sept. 23-27, 2018: IEEE, 2018. Pp. 6263-6269 Doi: 10.1109/ECCE.2018.8557497.

© 2018 IEEE. Es permet l'ús personal d'aquest material. S'ha de demanar permís a l'IEEE per a qualsevol altre ús, incloent la reimpressió/reedició amb fins publicitaris o promocionals, la creació de noves obres col·lectives per a la revenda o redistribució en servidors o llistes o la reutilització de parts d'aquest treball amb drets d'autor en altres treballs.

Cristian Verdugo, Mohamed Atef Elsharty, Pedro Rodríguez. (2018) Integrated series transformer in cascade converters for photovoltaic energy systems. ECCE 2018: IEEE Energy Conversion Congress and Exposition: Portland, OR, USA: Sept. 23-27, 2018: IEEE, 2018. Pp. 6263-6269 Doi: 10.1109/ECCE.2018.8557497.

© 2018 IEEE. Es permet l'ús personal d'aquest material. S'ha de demanar permís a l'IEEE per a qualsevol altre ús, incloent la reimpressió/reedició amb fins publicitaris o promocionals, la creació de noves obres col·lectives per a la revenda o redistribució en servidors o llistes o la reutilització de parts d'aquest treball amb drets d'autor en altres treballs.

Integrated Series Transformer in Cascade Converters for Photovoltaic Energy Systems

Cristian Verdugo

Department of Electrical Engineering
Polytechnic University of Catalonia
Terrassa, Spain

Email: cristian.andres.verdugo@upc.edu

Mohamed Atef Elsaharty

Department of Electrical Engineering
Polytechnic University of Catalonia
Terrassa, Spain

Email: mohamed.atef.abbas.elsaharty@upc.edu

Pedro Rodriguez

Department of Electrical Engineering
Loyola Andalusia University
Seville, Spain

Email: prodriguez@uloyola.es

Abstract—This paper proposes a novel configuration for photovoltaic applications based on a cascade converter topology. The series connection between modules is achieved through the magnetic core of the integrated series transformer, therefore an inherent isolation is provided without the requirement of a dc-dc conversion stage. Such isolation approach between each module allows operation at high voltage levels without harming the PV panel insulation. The main principles that support this proposal, as well as, simulation results are presented to validate the configuration.

I. INTRODUCTION

Among the different renewable energy sources, photovoltaic (PV) energy is one of the highly installed renewable source worldwide. The high demand of this energy has driven to develop better cost-competitive technologies to improve its characteristics and overcome the constraints over those that currently exist. Traditionally, PV systems are grouped in different type of configurations [1]: string topology (implemented in small and medium PV systems), multi-string topology (implemented in medium and large scale systems) and central configuration (implemented in large PV power plants). Currently, the most common topologies used by the inverter stage are the Neutral Point Clamped, the T-type converter and the H-Bridge converter.

For high power applications, PV panels are clustered into series and parallel connections to achieve the required dc voltage and current. However, the PV panel insulation defines the maximum dc voltage allowed by the series connection of panels (PV string) which can not surpass the voltage limit set by the manufacturer (1000V to 1500V). This voltage limit restricts PV systems to only operate at low voltage levels unless multi-cell converters are used to split the dc voltage and decrease the voltage stress [2]. Multi-cell converters are a subgroup of multilevel converters and consist of a series connection of modules which increase the voltage level operation as the number of modules increase. Using an appropriate modulation, the series connection increases the number of output voltage levels, yielding a reduction in the ac current ripple and thus, higher power quality and smaller ac filter requirements.

The cascade converter [2] is the conventional multi-cell configuration used in PV applications. Different control algorithms have been proposed to control this converter in several

scenarios. Although the modules split the voltage stress of the PV panels, PV insulation remains a problem in multi-cell converters if galvanic isolation is not considered. To provide this isolation, a dc-dc stage with a high frequency transformer is commonly used, in this way, the dc and the ac side are decoupled and it is possible to control their variables independently. Nevertheless, the requirement of two stages (the dc-dc converter and the inverter) increase the implementation cost, the control complexity and in some cases they are not a feasible option. Among the possible solutions to such a challenge is the use of multiple power transformers connected in series to achieve galvanic isolation between different modules. However, such an approach requires bulky transformers capable of handling the line current as well as this yields a larger setup footprint.

Integration of several transformers into a single monolithic structure has gained interest in recent literature. Such structures resolve converter galvanic isolation challenges as well as setup footprint limitations. The configuration discussed in [3], utilizes multiple series transformers with multi-secondary windings. In such a configuration, series compensation of each phase is distributed over several converters connected through a single series transformer. Multiple power electronics converters inject the corresponding secondary winding currents to achieve the required fundamental reference current. However, in this configuration, the equivalent circuit per phase results in multiple converters connected in shunt to each other through the series transformer which does not achieve a cascaded topology. Another approach of series converter integration is shown in [4] through a shunt magnetic path. The shunt magnetic path is inserted between the primary and secondary limbs to control the secondary voltage of the transformer. However, this approach has not been investigated for cascaded converter and power system applications.

For these reasons, this paper presents a novel configuration for cascade converters based on an integrated series transformer. The proposal provides a cascade converter with a galvanic isolation without the requirement of a dc-dc stage and high frequency transformer. The power transformer used is based on the configuration presented in [5], where it is shown the possibility of providing multiple series and shunt connections in a single integrated transformer. The Custom

Power Active Transformer (CPAT), [6], utilizes multiple shunt magnetic paths to provide equivalent series connections as well as multiple shunt connection between the primary and secondary side. Through the presented concept, simulations results validate the feasibility of such an integrated configuration

This paper is organized as follows: Section II introduces the proposed configuration and presents the theory of operation. In Section III a derivation of the transformer model is revealed and the analysis for the required operation principle is studied. Section IV discusses the utilized control strategy for the proposed integrated converter-transformer structure and in Section V the simulation results are evaluated. Finally, conclusions of the proposed approach are summarized in Section VI.

II. PROPOSED CONFIGURATION

The concept of an integrated series transformer is based upon the magnetic circuits theory presented in [7], which states that windings wound over shunt core limbs are equivalent to series electrical circuits. Using this concept, the CPAT discussed in [6] has proved the capability of integrating a series winding between primary and secondary side of a power transformer. As discussed earlier, to overcome the PV panels voltage limitation on the dc side, this integrated concept is utilized to form the required cascaded converter connection with galvanic isolation. The proposed configuration shown in Fig.1, presents three modules connected to each limb winding, while the grid is connected to the fourth limb winding. Even though, the configuration presented has three modules, the converter can be extended into more modules only by increasing the number of limbs in the transformer. Based on the approach in [6], each limb provides a shunt magnetic path. Since the magnetic flux is directly proportional to the applied voltage in a winding (i.e. $v_1 \propto \Phi_1$, $v_2 \propto \Phi_2$, $v_3 \propto \Phi_3$ and $v_4 \propto \Phi_4$), the sum of all magnetic fluxes would add up to zero since all elements are shunt connected in the magnetic circuit. Moreover, all limbs in Fig.1 are in shunt to each other, this entails that each limb would exhibit an equal magneto-motive force (i.e. $F_1 = F_2 = F_3 = F_4$) which is directly proportional to the current through a winding. In this way, the magneto-motive force across the transformer would increase/decrease depending on the power transferred in the transformer. It is worth to be noted that the transformer windings provide inherent filtering capability due to the winding inductance. Moreover, with such a configuration, there is no limitation to the dc bus voltage (V_{dc1} , V_{dc2} , V_{dc3}) variation between each module. Further explanation into the transformer model and theory of operation will be discussed in the next section.

The configuration is proposed for a single phase system, however, the converter can be extended to a three phase configuration, where it is only necessary to add two independent magnetic cores for each phase. Regarding to the inverter module, the topology used is irrelevant in this work, but for a sake of simplicity, a H-Bridge converter is used. Therefore, the series connection of modules increase the output voltage N times V_{dc} only if all modules operate at the same voltage level.

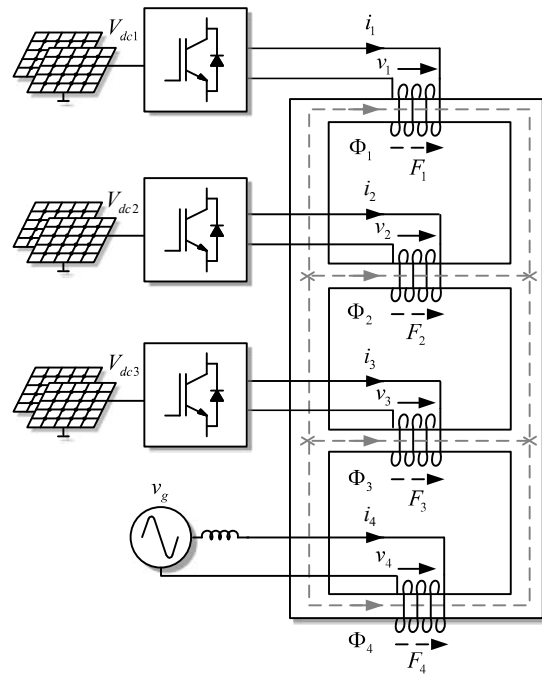


Fig. 1. Integrated series transformer in a cascade converter

However, this assumption could not be true if the PV string are affected by different temperature and radiation conditions and each module is controlled to operate at their maximum power point. In such a case, asymmetrical voltage levels could appear in the equivalent output voltage.

Each inverter module in Fig.1 operates at the Maximum Power Point (MPP) available from the connected PV panel using a Maximum Power Point Tracking (MPPT) technique. In this case, a single-stage MPPT technique [8],[9] can be utilized to derive the required output current from each inverter module. The magnetizing current required to energize each limb of the transformer consists of fractional odd order harmonics as discussed in [6]. However, such odd harmonics can be provided by each inverter module through appropriate current control of the inverter modules. The effect of the magnetizing current is not considered in this proposal since its analysis is outside the conceptual scope of this paper.

Depending on the modulation technique implemented, the H-Bridge can generate two or three output voltage levels [10]. The unipolar modulation controls each leg independently, hence $-V_{dc}$, 0 and V_{dc} are generated in the ac side. By using a phase shift modulation [11], it is possible to increase the number of output voltage levels and the apparent switching frequency observed in the grid current. Since unipolar modulation is implemented, by shifting $(i-1)\pi/N$ the carrier modulation in the module i , the output voltage levels increase up to $(2N+1)$ and the apparent switching frequency increase $2Nf_c$ times, where f_c is the carrier frequency.

III. TRANSFORMER MODEL DESCRIPTION

The principle discussed can be further extended to k number of series elements as shown in Fig.2. Each limb consists of N windings which are selected based on the transformation ratio of the injected voltage to the induced flux in the core. Considering that limbs 1,2... $k-1$ are connected to PV converter modules while the last limb k is connected to the grid, the voltage induced at the grid winding can be represented as in (1a). Meanwhile, since the structure represents an equivalent series circuit, the current in each winding (i_n) would be a fraction of the grid current (i_k) based on the turns ratio as presented in (1b).

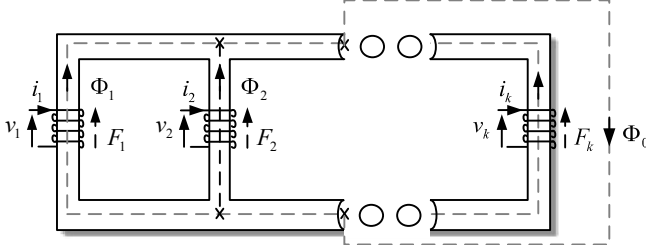


Fig. 2. Integrated series transformer

$$v_k = N_k \sum_{n=1}^{n=k-1} \frac{v_n}{N_n} \quad (1a)$$

$$i_n = i_k \frac{N_n}{N_k} \quad (1b)$$

To obtain a topologically correct equivalent model of the transformer presented in Fig.2, the equivalent magnetic circuit is derived by discretizing the magnetic flux paths in the core and air as shown in Fig.3. The magnetic circuit shown in Fig.3a consists of k limbs with winding fluxes Φ_k , core fluxes Φ_{ck} , winding leakage fluxes Φ_{Lk} and core leakage flux Φ_0 . Core limbs and yokes are represented by non-linear reluctances \mathfrak{R}_Y \mathfrak{R}_L with a value calculated based on the B-H characteristics of the core material. A non-linear reluctance is modeled as a controlled magneto-motive source in a closed-loop between input flux and output magneto-motive force (F) as shown in Fig.3b. This model would produce an opposing magneto-motive force based on the limb/yoke length (l), area (A) and the core B-H characteristics. Meanwhile, winding leakage reluctances (\mathfrak{R}_k) as well as core leakage reluctance (\mathfrak{R}_0) are represented by linear reluctances. Leakage reluctances are evaluated based on dimensions as in (2) using the flux path length, mean area and relative permeability of air ($\mu_0 = 4\pi 10^{-7}$). The flux generated by each winding is linked to a winding electric circuit shown in Fig.3c to model winding losses and core equivalent losses. For any applied winding voltage (v_k), the equivalent transformer winding currents (i_k) is dependent upon winding resistance (R_k), equivalent core loss resistance (R_c) and effective winding current (i_{ek}). The effective current is calculated based on the effective magneto-motive force (F_k) of the winding and number of turns (N_k)

as shown in Fig.3c. Whereas, the winding flux in the magnetic circuit is deduced from the effective voltage (v_{ek}) in the winding electric circuit.

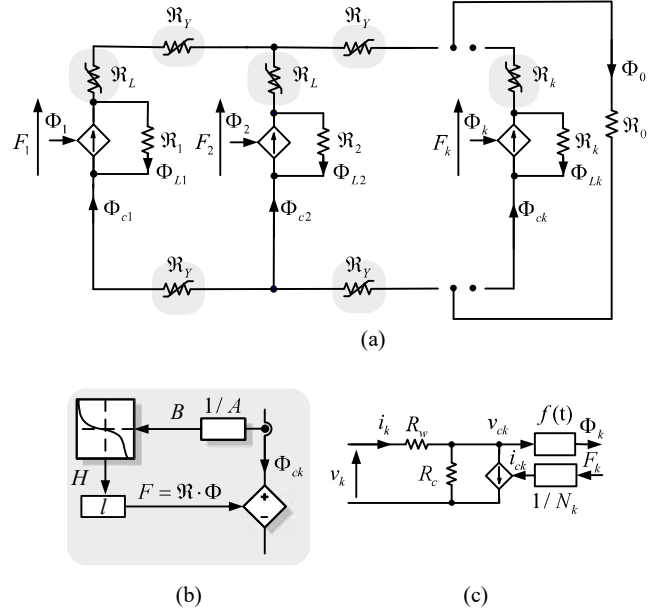


Fig. 3. Integrated series transformer model. (a) Equivalent magnetic circuit, (b) Reluctance model and (c) Winding and core losses in the electrical circuit

$$\mathfrak{R}_0 = \mathfrak{R}_k = \frac{l}{\mu A} \quad (2)$$

It is worth to be noted that to overcome algebraic loops due to the coupling between electric, magnetic and non-linear reluctance circuit, a one-simulation-step-time delay is applied. However, such an approach should be considered with high sampling-rate to avoid numerical oscillations.

Using duality transformation [12], the equivalent electric circuit shown in Fig.4a can be deduced from Fig.3 with non-linear and linear reluctances transformed into their equivalent inductance values. It can be observed that the equivalent electric circuit shown in Fig.4a consists of multiple series circuits which would develop the cascaded configuration of the converters upon connection. Assuming perfect coupling between windings, the equivalent core inductance (L_L, L_Y) can be considered significantly large compared to leakage inductance (L_k, L_0) and thus, the reduced equivalent electric circuit is represented by Fig.4b. The assumption that (L_L, L_Y) are significantly large is used to neglect the effect of magnetizing current on the performance of the system. However, magnetizing currents of each limb are dependent on the design of the transformer (limb length and area) and they can be compensated through appropriate current control of each inverter module as in [5].

IV. CONTROL STRATEGY

The grid current is controlled through the power provided by PV panels and the voltage levels required in the dc side.

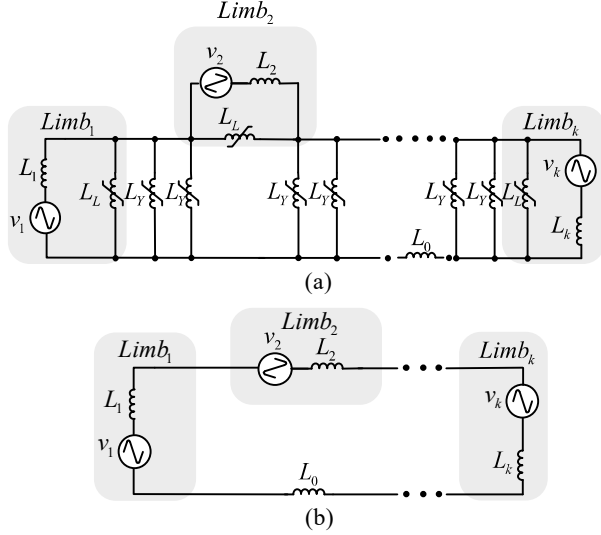


Fig. 4. Integrated series transformer. (a) Equivalent electric circuit, (b) Simplified electric circuit

The strategy used is based on the voltage oriented control architecture shown in Fig.5, where the average dc voltage provided by all modules is regulated to generate the ac current reference and then used to control the grid current through a PR controller. A MPPT algorithm [8] is implemented to extract the maximum power produced by PV panels connected in every module and the voltage reference given by this algorithm is subtracted from the dc voltage filtered at 100 Hz to control the total error in all modules. In order to synchronize the current reference and the grid current, a phase locked loop (PLL) [13] is used for proper synchronization. In this way, the active and reactive power depend on the synchronization angle θ_g .

The PR controller ensures zero steady state at the grid frequency, and the modulation index m provided by this control is used to control all modules. Since the external

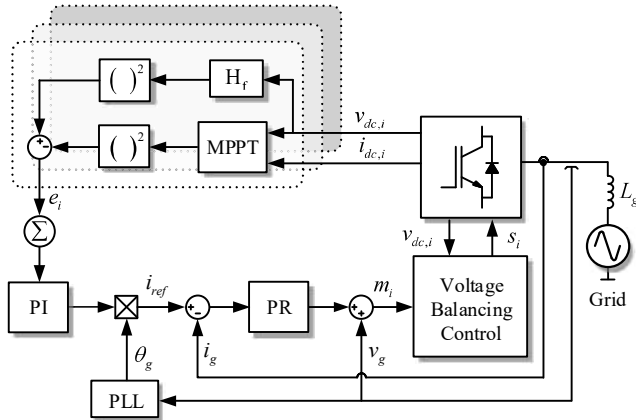


Fig. 5. Control strategy

dc voltage control loop regulates the average dc voltage, the power mismatching caused by different dc voltage levels will not be regulated unless a voltage balancing control responsible for adjusting the modulation index according to the dc voltage reference given by the MPPT algorithm is implemented.

The voltage balancing control used is based on the concept presented in [14], where the modulation index amplitude provided by the PR controller is adjusted according to the power level of each module. This modulation amplitude increase when the module is able to provide more power and decrease when the module reduces its maximum power level. The modulation adjustment is performed through a dc voltage control which regulates the new modulation index according to the next expression.

$$m_i^* = (1 - \Delta m_i) \cdot m \quad (3)$$

Where Δm_i is the control variable provided by the dc voltage control loop. In Fig.6 is shown the control scheme.

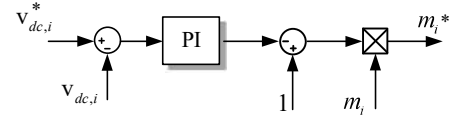


Fig. 6. Voltage balancing control

V. SIMULATION RESULTS

The proposed configuration and control scheme are validated through simulation results using Matlab/Simulink. The converter has three H-bridge modules connected to a four winding single-phase transformer with a nominal power of 6 kW split between all modules. The remaining parameters are listed in Table.I. In order to evaluate the performance of the proposed configuration, the converter is analyzed under symmetrical and asymmetrical scenarios with modules operating at equal and different power levels. In the first scenario, all modules generate the same power with the same dc voltage level. Therefore, the voltage balancing control does not adjust any modulation index. In the second and third scenario, there is a dc voltage changes in modules one and three. These events produce a power unbalance which is compensated through the voltage balancing control.

The simulation results are presented in Fig.7 to Fig.10. The dynamic dc voltage response of each module is shown in Fig.7, where it is observed how the dc voltage changes as the voltage reference decrease or increase. The first voltage step takes place at $t = 0.6$ s, in that time, all modules decrease their dc voltage reference from the open-circuit voltage to the voltage at maximum power level. Since all modules have the same physical characteristics, the dc voltage in Fig.7.a, Fig.7.b and Fig.7.c have the same dynamic. The previous scenario changes at $t = 1.4$ s, since the dc voltage in module 1 increase 35% regarding the previous level. This event causes a disturbance in the dc voltage of module 2 and module 3 as presented in

TABLE I
SIMULATION PARAMETERS

| Parameters | Symbol | Value |
|------------------------------|-------------|-----------------|
| Nominal power | P_o | 6 kW |
| Nominal power per module | P_M | 2 kW |
| Grid voltage amplitude | \hat{v}_g | 340 V |
| Grid frequency | f_s | 50 Hz |
| Open-circuit voltage | v_{oco} | 240 V |
| Voltage at maximum power | v_{mpp} | 140 V |
| DC-link capacitance | C_{dc} | 4700 μ F |
| DC resistor | R_{dc} | 4.33 Ω |
| Switching frequency | f_c | 2200 Hz |
| Grid inductance LC filter | L_g | 1 mH |
| Grid capacitance LC filter | C_g | 5 μ F |
| Transformer voltage | V_t | 400 V |
| Transformer power | P_t | 8 kW |
| Inductance primary winding | L_p | 0.9113 mH |
| Inductance secondary winding | L_s | 0.9113 mH |
| Resistance primary winding | R_p | 0.2518 Ω |
| Resistance secondary winding | R_s | 0.2518 Ω |
| Magnetizing inductance | L_m | 2 H |
| Base voltage | V_B | 240 V |
| Base power | S_B | 6 kW |
| Base current | I_B | 23.085 A |

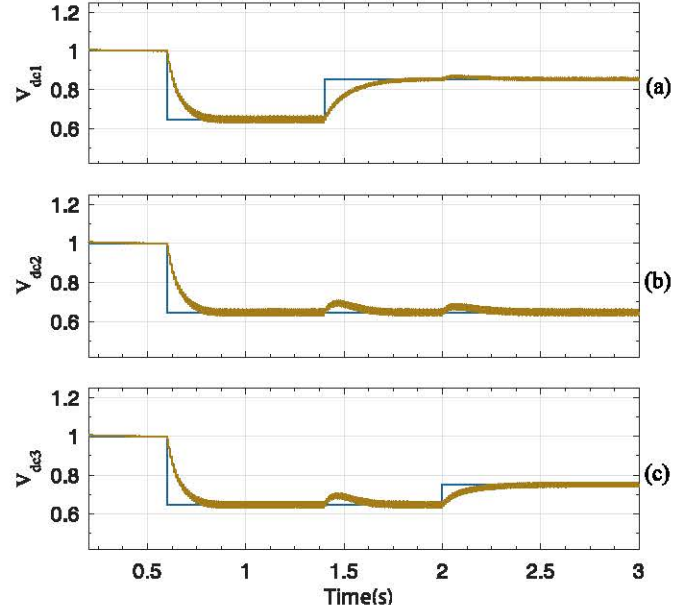


Fig. 7. Dynamic response of the dc voltage. (a) Module 1, (b) Module 2, (c) Module 3

Fig.7.b and Fig.7.c. The last dc voltage step takes place at $t = 2$ s, where the voltage of module 3 increase 15%.

The scenarios can also be analyzed according to the active power response shown in Fig.8. Since the first 0.6 s, all modules operate at open voltage circuit, the converter does not provide any power. After $t = 0.6$ s, all modules generate their maximum power available until $t = 1.4$ s, where the module 1 reduce its power. This state remains constant until $t = 2$ s, where the third module reduce its power 15%. Fig.8.d shows the the total power injected into the grid, and it is observed how the active power is reduced as the power provided by each module decrease.

In order to evaluate the grid synchronization and the voltage balancing control, in Fig.9 is shown the grid voltage, the grid current and the modulation index according to the time span marked in Fig.8. In Fig.9.a it is observed the synchronization between the grid voltage and grid current. Since, both signals are in phase, the power injected does not have any reactive power component. Note the voltage and current amplitude have different amplitude levels despite both signals are in per unit. This is because the power unbalance presented in all modules provide a total power level lower than the nominal value. On the other hand, the power mismatching among all modules has to be controlled to avoid over or under dc voltages and allow each module to operate at their voltage references. Because of this, the voltage balancing control adjusts the modulation index amplitude according to the dc voltage level. In Fig.9.b is shown the modulation index of each module, and it is observed that the second module has the highest modulation index amplitude, while the first module has the lowest amplitude. This difference between the modulation index amplitude corroborates the performance of the control

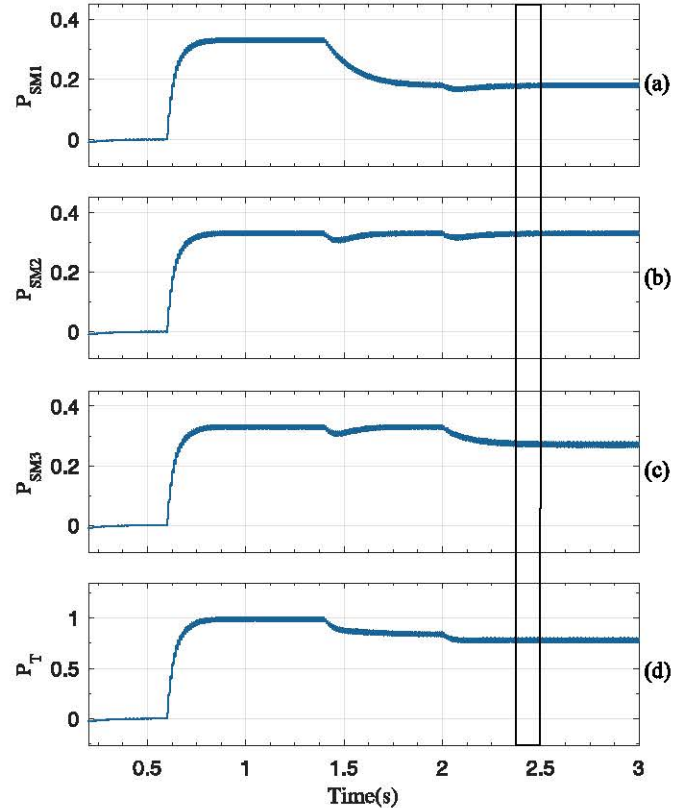


Fig. 8. Dynamic response of the active power. (a) Module 1, (b) Module 2, (c) Module 3, (d) Grid.

strategy, where the module with lower dc voltage is able to provide more power and thus, it requires a higher amplitude.

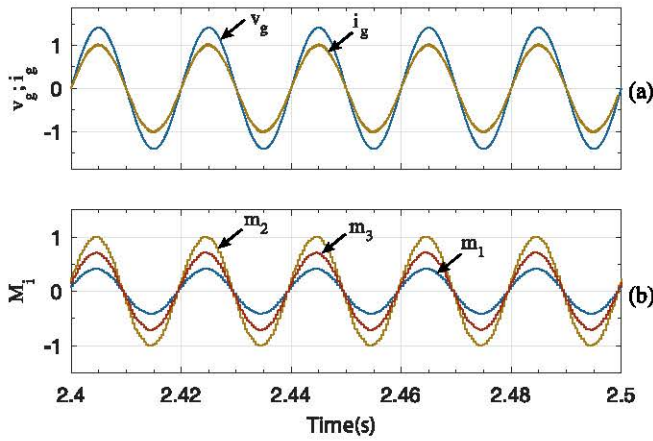


Fig. 9. Voltage, current and modulation index waveforms under unbalance operation. (a) Grid voltage and grid current, (b) Modulation index of all modules.

To validate more insights on the proposed configuration, the steady state response of the voltage at the ac side of each module and the voltage in the terminals of the fourth limb winding before the unbalance operation takes place are shown in Fig.10. The series connection provided by the magnetic core and the Level Shifted PWM modulation give rise to an increase of voltage levels in the fourth limb winding. Since three modules are used, the voltage at the fourth limb shown in Fig.10.d has seven levels, while each module has three levels. This characteristic allows a reduction of the grid filter requirements maintaining a low current ripple in the grid current.

VI. CONCLUSION

A novel configuration using an integrated series transformer has been proposed for cascade converters. Since the series connection is performed through the magnetic core, isolation of inverter modules for PV applications is provided without the requirement of a dc-dc conversion stage. This feature has presented many benefits over conventional configurations with respect to cost and control complexity. Based on the presented analysis and model, the proposed configuration has revealed that it is possible to achieve series connection of inverter modules using several shunt limbs in a single integrated transformer. Through the presented simulation results, the performance of the proposed conceptual configuration has been validated. However, for large scale implementation, it is necessary to consider the transformer non-linear parameters. This is in order to account for magnetizing currents as well as power losses in the design. Future research in such a configuration would include a deeper analysis of the converter under different scenarios and a detailed design of the transformer to account these parameters.

ACKNOWLEDGMENT

This project has been partially funded by the Spanish Ministry of Economy, Industry and Competitiveness under the

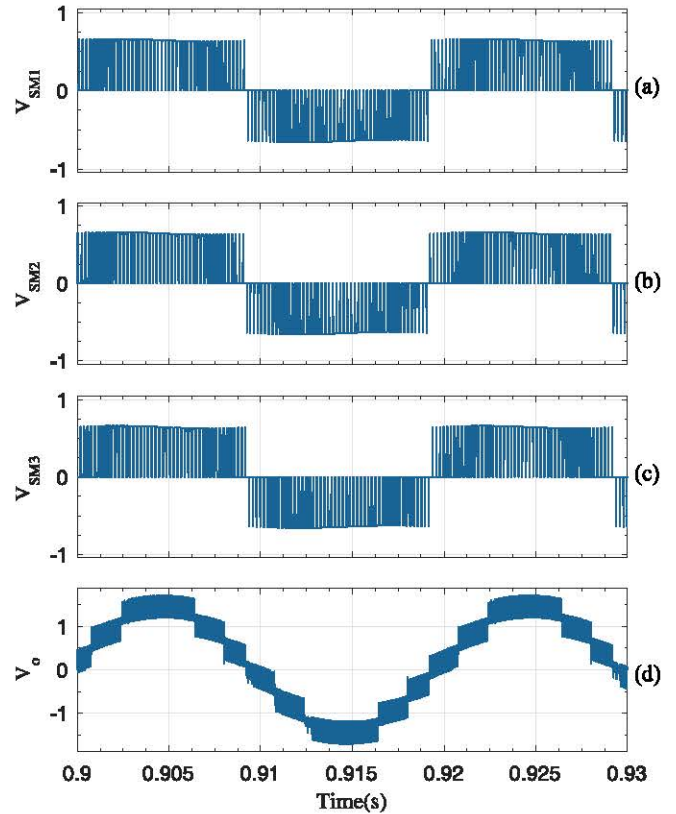


Fig. 10. Output voltage in steady state operation. (a) Module 1, (b) Module 2, (c) Module 3, (d) fourth limb winding

projects ENE2017-88889-C2-1-R and ENE206-79493-R

REFERENCES

- [1] S. B. Kjaer, J. K. Pedersen and F. Blaabjerg, "A review of single-phase grid-connected inverters for photovoltaic modules," in *IEEE Transactions on Industry Applications*, vol. 41, no. 5, pp. 1292-1306, Sept.-Oct. 2005.
- [2] S. Kouro, B. Wu, . Moya, E. Villanueva, P. Correa and J. Rodriguez, "Control of a cascaded H-bridge multilevel converter for grid connection of photovoltaic systems," 2009 35th Annual Conference of IBBE Industrial Electronics, Porto, 2009, pp. 3976-3982.
- [3] Dayi Li, Qiaofu Chen, Zhengchun Jia and Changzheng Zhang, "A high-power active filtering system with fundamental magnetic flux compensation," *IEEE Trans. Power Del.*, vol. 21, no. 2, pp. 823830, Apr. 2006.
- [4] Richard M. Hutchison, Don J. Corrigan, Shunt coil controlled transformer, Patent US5187428 A, Feb. 16, 1993.
- [5] M. A. Elsharty, J. I. Candela and P. Rodriguez, "Custom Power Active Transformer for Flexible Operation of Power Systems," in *IEEE Transactions on Power Electronics*, vol. PP, no. 99, pp. 1-1.
- [6] M. A. Elsharty, J. Rocabert, I. Candela and P. Rodriguez GAE, "Three-Phase Custom Power Active Transformer for Power Flow Control Applications," in *IEEE Transactions on Power Electronics*.
- [7] Yim-Shu Lee, Leung-Pong Wong and D. K. W. Cheng, "Simulation and design of integrated magnetics for power converters," *IEEE Trans. Magn.*, vol. 39, no. 2, pp. 1008-1018, Mar. 2003.
- [8] N. Femia, G. Petrone, G. Spagnuolo and M. Vitelli, "Optimization of perturb and observe maximum power point tracking method," in *IEEE Transactions on Power Electronics*, vol. 20, no. 4, pp. 963-973, July 2005.
- [9] H. Patel and V. Agarwal, "Maximum Power Point Tracking Scheme for PV Systems Operating Under Partially Shaded Conditions," in *IEEE Transactions on Industrial Electronics*, vol. 55, no. 4, pp. 1689-1698, April 2008.

- [10] D. Grahame Holmes; Thomas A. Lipo, "Appendix 3: ThreePhase and HalfCycle Symmetry Relationships," in *Pulse Width Modulation for Power Converters:Principles and Practice* , 1, Wiley-IEEE Press, 2003, pp.744-
- [11] D. G. Holmes and B. P. McGrath, "Opportunities for harmonic cancellation with carrier-based PWM for a two-level and multilevel cascaded inverters," in *IEEE Transactions on Industry Applications*, vol. 37, no. 2, pp. 574-582, Mar/Apr 2001.
- [12] S. Jazebi et al., "Duality Derived Transformer Models for Low-Frequency Electromagnetic TransientsPart I: Topological Models, *IEEE Trans. Power Del.*, vol. 31, no. 5, pp. 2410-2419, Oct. 2016.
- [13] P. Rodriguez, J. Pou, J. Bergas, J. I. Candela, R. P. Burgos and D. Boroyevich, "Decoupled Double Synchronous Reference Frame PLL for Power Converters Control," in *IEEE Transactions on Power Electronics*, vol. 22, no. 2, pp. 584-592, March 2007.
- [14] C. Verdugo, S. Kouro, M. A. Perez, M. Malinowski and T. Meynard, "Series-connected T-type Inverters for single-phase grid-connected Photovoltaic Energy System," *IECON 2013 - 39th Annual Conference of the IEEE Industrial Electronics Society*, Vienna, 2013, pp. 7021-7027.
- lectronics, vol. 20, no. 4, pp. 963-973, July 2005.